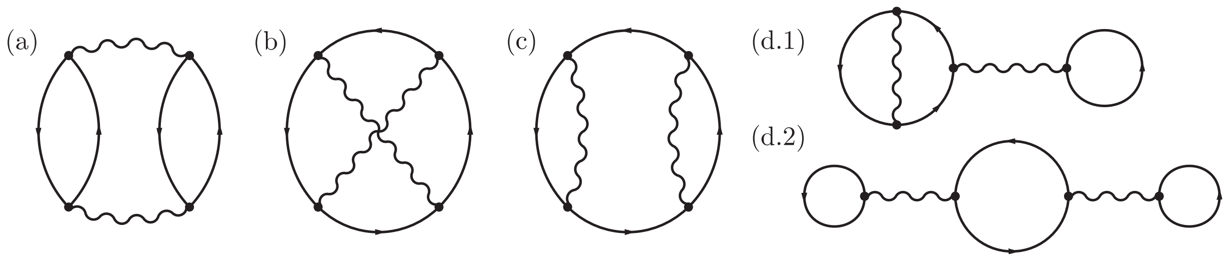

FIG. 4: Diagrams for the second order in the fermion language. Interesting low-energy contributions are only due to diagrams (a) and (b) whereas diagram (c) just renormalize the chemical potential. To check the equivalence of the bosonized model to the original fermion one, we must check, however, that all fermion diagrammatic contributions are exactly reproduced.

are important for low-energy physics, whereas the diagram (c) merely modifies the chemical potential. The diagrams 4 (d.1) and (d.2) contain the Hartree bubbles that also result in a renormalization of the chemical potential.

Nevertheless, in order to understand details it is important to obtain *all* contributions of the perturbation theory for the boson superfield theory. Checking the exact correspondence between the original fermion and the boson models is what this Section is devoted to.

Before presenting the details of the calculations, let us make some general remarks. For $\hat{H}^{(1)}_{int}$ [Eq. (2.8)], the Hartree-type contributions 4 (d.1) and 4 (d.2) are in the boson theory generally accounted for by the renormalization of the chemical potential [Eq. (2.14)] and by the trivial contribution to the thermodynamic potential in Eq. (2.13). There is no contribution of diagrams containing closed loops of boson propagators because they vanish due to the superfield symmetry. The effective second order diagrams in the bosonized theory are shown in Fig. 5.

Drawing parallels with the conventional fermion diagrams we interpret the double-lines in Fig. 5 as pairs of single fermion propagator lines. This is similar to what we successfully did when discussing the first order diagrams. In this spirit, inspection of the diagrams suggests that the conventional RPA diagram Fig. 4 (a) is reproduced in the boson language by Fig. 5 (a), the correlation diagram Fig. 4 (b) by Figs. 5 (b.4,c.1), and, finally, the conventional diagram with the two Fock loops, Fig. 4 (c), by Figs. 5 (b.1-b.3,c.2). However, for contributions coming from the on-site interaction Hamiltonian $\hat{H}^{(0)}_{int}$ [Eq. (2.8)], this "graphical picture" describes the correspondence in a less strict way since the conventional diagrams (a) and (b) as well as the conventional diagrams (c), (d.1), and (d.2) in Fig. 4 coincide in this case, thus making a parallel between just Fig. 4 (a) and Fig. 5 (a) meaningless. In this case one can speak only about a "weaker" correspondence between Figs. 4 (a,b) and Figs. 5 (a,b.4,c.1,c.2).

Having established these parallels, the detailed calculations can be performed in an organized manner, which is straightforward though a little tedious.

Starting with $\langle {\mathcal{S}_2}^2 \rangle$, the evaluation of the diagram in Figs. 5 (a) yields

$$
\begin{aligned}
\langle {\mathcal{S}_2}^2 \rangle &= -2N_d \sum_{\omega} \int \left(V_{\mathbf{q}}^2 - 2V_0V_{\mathbf{q}} + 2V_0^2\right)[n_{\mathbf{p}+\mathbf{q}} - n_{\mathbf{p}}] \\
&\quad \times [n_{\mathbf{p}'+\mathbf{q}} - n_{\mathbf{p}'}] g(\omega,\mathbf{p}+\mathbf{q},\mathbf{p}) g(\omega,\mathbf{p}'+\mathbf{q},\mathbf{p}')(d\mathbf{p}d\mathbf{p}'d\mathbf{q}), \\
&= 2N_dT^2 \sum_{\varepsilon\varepsilon'\omega} \int V_{\mathbf{q}}^2 G^0_{\varepsilon,\mathbf{p}+\mathbf{q}} G^0_{\varepsilon+\omega,\mathbf{p}} \\
&\quad \times G^0_{\varepsilon',\mathbf{p}'+\mathbf{q}} G^0_{\varepsilon'+\omega,\mathbf{p}'}(d\mathbf{p}d\mathbf{p}'d\mathbf{q}) \qquad (3.26a) \\
&\quad + 2N_dT^2 \sum_{\varepsilon\omega\omega'} \int (-2V_0V_{\mathbf{q}} + 2V_0^2) G^0_{\varepsilon,\mathbf{p}} G^0_{\varepsilon+\omega,\mathbf{p}+\mathbf{q}} \\
&\quad \times G^0_{\varepsilon+\omega+\omega',\mathbf{p}+\mathbf{q}+\mathbf{q}'} G^0_{\varepsilon+\omega',\mathbf{p}+\mathbf{q}'}(d\mathbf{p}d\mathbf{q}d\mathbf{q}') \qquad (3.26b)
\end{aligned}
$$

where Eq. (2.35) has been applied and the notation $G^0_{\varepsilon,\mathbf{p}} = (i\varepsilon - \xi_{\mathbf{p}})^{-1}$ for the fermion Green function in the original electron language is used, $\xi_{\mathbf{p}} = \varepsilon_{\mathbf{p}} - \mu$. In the second term (3.26b), the momenta in the Green functions have been shifted using the fact that at least one of the involved interaction couplings V is independent of the running momentum $\mathbf{q}$ (on-site interaction).

Inspection of the expressions obtained shows that the first term (3.26a) is indeed identical to the conventional second order RPA contribution, Fig. 4 (a). This one-to-one correspondence of the $V_{\mathbf{q}}^2$-term confirms the validity of the "graphical correspondence". The form of the second term resembles the contribution of the diagram Fig. 4 (b) and therefore we expect that it should be cancelled by those diagrams of $\langle {\mathcal{S}_3}^2 \rangle$ and $\langle \mathcal{S}_2\mathcal{S}_4 \rangle$ that we have already related to the conventional contribution of Fig. 4 (b). Since for the purely on-site interaction the diagrams Fig. 4 (a) and (b) are indistinguishable, there is no surprise that $\langle {\mathcal{S}_2}^2 \rangle$ also contributes to the conventional diagram in Fig. 4 (b) due to the presence of the $\hat{H}^{(0)}_{int}$-channel, Eq. (2.8).

So, let us consider now the boson diagrams shown in Figs. 5 (b.4,c.1) which are of conventional type of Fig. 4 (b) in terms of their graphical shape. Their eval-